Supporting Information; Swimming microorganisms acquire optimal efficiency with multiple cilia

Toshihiro Omori[a], **Hiroaki Ito**[a], **and Takuji Ishikawa**[a,b]

[a]Department of Finemechanics, Tohoku University, Japan; [b]Department of Biomedical Engineering, Tohoku University, Japan

Governing equations and numerical methods

Here, we explain governing equations and numerical methods. Details can be also found in our published paper (1).

Boundary integral equation with slender body theory. Consider a ciliate immersed in an infinite Newtonian liquid of density ρ and viscosity μ; the ciliate is propelled via individual ciliary motion. The inertial effect of fluid flow is negligible; the Reynolds numbers scaled by ciliary motion and swimming are markedly lower than 1 ($Re \ll 1$). Thus, fluid flow around the ciliate is governed by the Stokes equation. The cell body is modelled as a rigid spheroid from which cilia emerge. As cilia are slender, slender-body theory is applicable when analysing ciliary motion. We parameterise the ciliary centreline using archlength $s \in [0, L]$, where L is the ciliary length. The flow field at point $\boldsymbol{x}$ is located on the i-th cilium, $\boldsymbol{x} \in s_i$, is given by (1, 2):

$$\begin{aligned} \boldsymbol{v}(\boldsymbol{x}) &= -\frac{1}{8\pi\mu}\int_{cell} \boldsymbol{J}(\boldsymbol{x},\boldsymbol{y})\cdot\boldsymbol{q}(\boldsymbol{y})dA(\boldsymbol{y}) - \frac{1}{8\pi\mu}\boldsymbol{\Lambda}(\boldsymbol{x})\cdot\boldsymbol{f}(\boldsymbol{x}) \\ &\quad -\frac{1}{8\pi\mu}\int_{cilia} \left[\boldsymbol{J}(\boldsymbol{x},\boldsymbol{y})\cdot\boldsymbol{f}(\boldsymbol{y}) + \boldsymbol{K}(\boldsymbol{x},\boldsymbol{y})\cdot\boldsymbol{f}(\boldsymbol{x})\right] ds_i(\boldsymbol{y}) \\ &\quad -\frac{1}{8\pi\mu}\sum_{j\neq i}^{N}\int_{cilia} \left[\boldsymbol{J}(\boldsymbol{x},\boldsymbol{y}) + \boldsymbol{W}(\boldsymbol{x},\boldsymbol{y})\right]\cdot\boldsymbol{f}(\boldsymbol{y})ds_j(\boldsymbol{y}), \end{aligned} \quad [1]$$

where $\boldsymbol{q}$ is the viscous traction on the cell body, $\boldsymbol{f}$ is the force density per unit length, and N is the total number of cilia. The first integral on the right operates over the entire spheroidal cell surface, and the second and third integrals operate along the central ciliary lines. $\boldsymbol{J}$ is Green's function, as given by:

$$J_{ij}(\boldsymbol{x},\boldsymbol{y}) = \frac{\delta_{ij}}{r} + \frac{r_i r_j}{r^3}, \quad [2]$$

where $r = |\boldsymbol{r}|$, $\boldsymbol{r} = \boldsymbol{x} - \boldsymbol{y}$. $\boldsymbol{\Lambda}$ and $\boldsymbol{K}$ are the local operators of the slender body theory, which are given by:

$$\Lambda_{ij}(\boldsymbol{x}) = c\left[\delta_{ij} + t_i(\boldsymbol{x})t_j(\boldsymbol{x})\right] + 2\left[\delta_{ij} - t_i(\boldsymbol{x})t_j(\boldsymbol{x})\right], \quad [3]$$

and

$$K_{ij}(\boldsymbol{x},\boldsymbol{y}) = -\frac{\delta_{ij} + t_i(\boldsymbol{x})t_j(\boldsymbol{x})}{|s(\boldsymbol{x}) - s(\boldsymbol{y})|}, \quad [4]$$

where $c = -\ln(\varepsilon^2 e)$, $\boldsymbol{t}$ is the unit tangential vector to the centreline of each cilium and $\varepsilon = a_{cilia}/L$, and a_{cilia} is the ciliary radius. In terms of the practical ciliary radius and length ratio, the slenderness value ε is set to $\varepsilon = 0.01$. The slender body kernel $\boldsymbol{W}$ is defined by:

$$W_{ij}(\boldsymbol{x},\boldsymbol{y}) = \frac{(\varepsilon L)^2}{2}\left(\frac{\delta_{ij}}{r^3} - 3\frac{r_i r_j}{r^5}\right). \quad [5]$$

When the observation point $\boldsymbol{x}$ is not on a cilium, $\boldsymbol{x} \notin s$, the velocity is given by

$$\begin{aligned} \boldsymbol{v}(\boldsymbol{x}) &= -\frac{1}{8\pi\mu}\int_{cell} \boldsymbol{J}(\boldsymbol{x},\boldsymbol{y})\cdot\boldsymbol{q}(\boldsymbol{y})dA(\boldsymbol{y}) \\ &\quad -\frac{1}{8\pi\mu}\sum_{j=1}^{N}\int_{cilia} \left[\boldsymbol{J}(\boldsymbol{x},\boldsymbol{y}) + \boldsymbol{W}(\boldsymbol{x},\boldsymbol{y})\right]\cdot\boldsymbol{f}(\boldsymbol{y})ds_j(\boldsymbol{y}). \end{aligned} \quad [6]$$

Though the asymptotic accuracy of kernels $\boldsymbol{\Lambda}$ and $\boldsymbol{K}$ is $\mathcal{O}(\varepsilon^2 \ln \varepsilon)$, kernel $\boldsymbol{W}$ is accurate only to the limit $\mathcal{O}(\varepsilon)$. The equations [1] and [6] are therefore accurate to the limit $\mathcal{O}(\varepsilon)$.

Table 1. Fourier coefficients for ciliary beating, which are taken from Fulford and Blake (3).

$[A^1_{mn}]$	n	0	1	2	3	$[A^2_{mn}]$	0	1	2	3
	1	-0.654	0.393	-0.097	0.079		1.895	-0.018	0.158	0.010
m	2	0.787	-1.516	0.032	-0.302		-0.552	-0.126	-0.341	0.035
	3	0.202	0.716	-0.118	0.142		0.096	0.263	0.186	-0.067
$[B^1_{mn}]$	n	1	2	3		$[B^2_{mn}]$	1	2	3	
	1	0.284	0.006	-0.059			0.192	-0.050	0.012	
m	2	1.045	0.317	0.226			-0.499	0.423	0.138	
	3	-1.017	-0.276	-0.196			0.339	-0.327	-0.114	

Ciliary motions. We first define an orthonormal frame for the cell body $\boldsymbol{e}_i$ with origin $\boldsymbol{x}_c$, where $\boldsymbol{x}_c$ is the body mass centre; $\boldsymbol{e}_1$ then reflects swimming orientation. To efficiently model ciliary motion on the cell surface, local vectors with an orthonormal basis $\boldsymbol{g}_i$ are defined as follows. A material point $\boldsymbol{x}_b$, located at the base of a cilium on the cell surface, serves as the origin of the orthonormal body frame $\boldsymbol{g}_i$. The basis vectors $\boldsymbol{g}_1$ and $\boldsymbol{g}_2$ are defined as: $\boldsymbol{g}_1(\boldsymbol{x}_b) = \boldsymbol{b}(\boldsymbol{x}_b) \wedge \boldsymbol{n}(\boldsymbol{x}_b)/|\boldsymbol{b}(\boldsymbol{x}_b) \wedge \boldsymbol{n}(\boldsymbol{x}_b)|$ and $\boldsymbol{g}_2(\boldsymbol{x}_b) = \boldsymbol{n}(\boldsymbol{x}_b)$, where $\boldsymbol{b} = \boldsymbol{e}_1 \wedge \boldsymbol{n}$ and $\boldsymbol{n}$ is the outward unit normal vector, respectively. The time-dependent profile of each ciliary motion is derived using the following mathematical formula of Fulford and Blake (3):

$$\boldsymbol{x}^{cilia}(\boldsymbol{x}_b, s, t) = \xi^1(s,t)\boldsymbol{g}_1(\boldsymbol{x}_b) + \xi^2(s,t)\boldsymbol{g}_2(\boldsymbol{x}_b), \tag{7}$$

where

$$\xi^i(s,t) = \frac{1}{2}\alpha^i_0(s) + \sum_{n=1}^{N_0} \alpha^i_n(s)\cos n\omega t + \beta^i_n(s)\sin n\omega t, \tag{8}$$

ω is the angular beat frequency. The Fourier coefficients α^i_n and β^i_n are given by

$$\alpha^i_n(s) = \sum_{m=1}^{M_0} A^i_{mn} s^m, \quad \beta^i_n(s) = \sum_{m=1}^{M_0} B^i_{mn} s^m. \tag{9}$$

The coefficients A^i_{mn} and B^i_{mn} are summarized in table 1. In this study, the wave numbers N_0 and M_0 are set to 3. The parameters for ciliary beating are shown in table 1.

Boundary element method. In order to simulate free-swimming of the ciliate model, force-free and torque-free conditions are taken into account:

$$\int_{cell} \boldsymbol{q}\, dA + \sum_{i=1}^{N} \int_{cilia} \boldsymbol{f} ds_i = 0, \tag{10}$$

and

$$\int_{cell} \boldsymbol{q} \wedge \hat{\boldsymbol{r}} dA + \sum_{i=1}^{N} \int_{cilia} \boldsymbol{f} \wedge \hat{\boldsymbol{r}} ds_i = 0, \tag{11}$$

where $\hat{\boldsymbol{r}} = \boldsymbol{x} - \boldsymbol{x}_c$, and $\boldsymbol{x}_c$ is the mass center of the cell body.

Assume that the cell body shows a rigid motion, velocity on the spheroidal cell body surface and on the cilia can be expressed by:

$$\begin{aligned} &\boldsymbol{v}(\boldsymbol{x}) = \boldsymbol{U} + \boldsymbol{\Omega} \wedge \hat{\boldsymbol{r}}(\boldsymbol{x}), && \boldsymbol{x} \in \text{cell body} \\ &\boldsymbol{v}(\boldsymbol{x}) = \boldsymbol{U} + \boldsymbol{\Omega} \wedge \hat{\boldsymbol{r}}(\boldsymbol{x}) + \boldsymbol{v}^{cilia}(\boldsymbol{x}), && \boldsymbol{x} \in \text{cilia} \end{aligned} \tag{12}$$

where $\boldsymbol{U}$ is the translational and $\boldsymbol{\Omega}$ the angular velocity. $\boldsymbol{v}^{cilia}$ is the ciliary velocity with respect to the body frame $\boldsymbol{e}_i$ (i.e. $\boldsymbol{v}^{cilia} = \partial \boldsymbol{x}^{cilia}/\partial t$). We then solve the resistance problem with respect to the unknown $\boldsymbol{U}$, $\boldsymbol{\Omega}$, and derive the viscous tractions $\boldsymbol{q}$ and $\boldsymbol{f}$. We note that the angular velocity $\boldsymbol{\Omega}$ is almost zero in the present study due to the axisymmetry of the problem.

The cell body is modelled as a rigid spheroid, and the body surface discretised into 5,120 triangular mesh elements with 2,562 nodal points. Each cilium is discretised into 16 nodes that are interpolated using the centripetal Catmull-Rom spline method. All physical quantities are computed at each discretised point. The boundary integrals of [1] and [6] are computed

T. Omori
E-mail: omori@bfsl.mech.tohoku.ac.jp

with the aid of numerical Gaussian integration. When an observation point $\boldsymbol{x}$ is located on the cell body, the following linear algebraic equation can be derived from [6]:

$$\left[\boldsymbol{v}^b\right] = \left[\mathcal{J}^{bb}\right][\boldsymbol{q}] + \left[\mathcal{J}^{bc}\right][\boldsymbol{f}]\,. \tag{13}$$

When $\boldsymbol{x}$ is on the cilia, on the other hand, we have the following equation from [1]:

$$[\boldsymbol{v}^c] = \left[\mathcal{J}^{cb}\right][\boldsymbol{q}] + [\mathcal{J}^{cc}][\boldsymbol{f}]\,. \tag{14}$$

The vector size of $\left[\boldsymbol{v}^b\right]$ and $[\boldsymbol{q}]$ are $3N_b$, while $[\boldsymbol{v}^c]$ and $[\boldsymbol{f}]$ have the size of $3N_c$, where N_b is the number of nodes on the cell body, and N_c is the total number of nodes on the cilia. The matrix size of $\left[\mathcal{J}^{bb}\right]$ and $\left[\mathcal{J}^{bc}\right]$ are $3N_b \times 3N_b$ and $3N_b \times 3N_c$, whereas $\left[\mathcal{J}^{cb}\right]$ and $[\mathcal{J}^{cc}]$ are $3N_c \times 3N_b$ and $3N_c \times 3N_c$, respectively. In the similar manner, discretized forms of force-torque conditions, Eqs.[10] and [11], can be written as:

$$\left[\mathcal{F}^b\right][\boldsymbol{q}] + [\mathcal{F}^c][\boldsymbol{f}] = [\boldsymbol{0}]\,, \tag{15}$$

and

$$\left[\mathcal{T}^b\right][\boldsymbol{q}] + [\mathcal{T}^c][\boldsymbol{f}] = [\boldsymbol{0}]\,. \tag{16}$$

Considering the boundary condition of [22], the system can be expanded to

$$\begin{bmatrix} \mathcal{J}^{bb} & \mathcal{J}^{bc} & \mathcal{U}^b & \mathcal{A}^b \\ \mathcal{J}^{cb} & \mathcal{J}^{cc} & \mathcal{U}^c & \mathcal{A}^c \\ \mathcal{F}^b & \mathcal{F}^c & \boldsymbol{0} & \boldsymbol{0} \\ \mathcal{T}^b & \mathcal{T}^c & \boldsymbol{0} & \boldsymbol{0} \end{bmatrix} \begin{bmatrix} \boldsymbol{q} \\ \boldsymbol{f} \\ \boldsymbol{U} \\ \boldsymbol{\Omega} \end{bmatrix} = \begin{bmatrix} \boldsymbol{0} \\ \boldsymbol{v}^{cilia} \\ \boldsymbol{0} \\ \boldsymbol{0} \end{bmatrix}. \tag{17}$$

The matrix components $\mathcal{U}^b$ and $\mathcal{A}^b$ are of sizes $3N_b \times 3$, whereas $\mathcal{U}^c$ and $\mathcal{A}^c$ are both $3N_c \times 3$. The dense matrix [17] is solved using the lower-upper (LU) factorisation technique. Given the translational and angular velocities, all material points are updated using the second-order Runge-Kutta method.

Parameter setting. In a Stokes flow regime, the fluid viscosity is simply a multiplier of both force and traction. The viscosity μ can be assumed to be unity, without loss of generality. We further assumed that all cilia exhibited identical beat frequencies, and beat periodically during computation. To express phase differences among ciliary beats on the cell surface (i.e. metachronal waves), the initial ciliary beat phase $\psi^0(\theta)$ was defined as:

$$\psi^0/2\pi = \sin(k\theta/2), \tag{18}$$

where k is the wave number in the θ direction. $\theta = [0, \pi]$ is the angle between the orientation vector $\boldsymbol{e}_1$ and $\hat{\boldsymbol{r}}_b$; and $\theta = \cos^{-1}(\boldsymbol{e}_1 \cdot \hat{\boldsymbol{r}}_b)$, where $\hat{\boldsymbol{r}}_b = (\boldsymbol{x}_b - \boldsymbol{x}_c)/|\boldsymbol{x}_b - \boldsymbol{x}_c|$. If k is positive, an antiplectic metachronal wave is in play; a symplectic metachronal wave is triggered by a negative k. When k is set to zero, all cilia beat in phase. For the antipletic wave, we set $k = 1$, whereas $k = -1$ for the symplectic wave. For all computations, the time interval Δt was set to $\Delta t/T = 0.01$, where T is the ciliary beat period.

Mechanical power. Once all unknowns $\boldsymbol{U}$, $\boldsymbol{\Omega}$, $\boldsymbol{q}$, and $\boldsymbol{f}$ are given, we can calculate the mechanical power under free swimming condition. The mechanical power is given by

$$P = \int \boldsymbol{q} \cdot (\boldsymbol{U} + \boldsymbol{\Omega} \wedge \hat{\boldsymbol{r}}) dA + \sum_i^N \int \boldsymbol{f} \cdot (\boldsymbol{U} + \boldsymbol{\Omega} \wedge \hat{\boldsymbol{r}} + \boldsymbol{v}^{cilia}) ds_i. \tag{19}$$

Drag force. Drag force of the ciliate can be calculated by the translation of the same shaped object. The boundary conditions are $\boldsymbol{v}^{cilia} = 0$ and $\boldsymbol{v}(\boldsymbol{x}) = \boldsymbol{U}$ for all $\boldsymbol{x} \in S$, where $\boldsymbol{U}$ is the translational velocity, and S is the ciliate' surface including cilia. Then, we solve the following equation with respect to $\boldsymbol{q}$ and $\boldsymbol{f}$:

$$\begin{bmatrix} \mathcal{J}^{bb} & \mathcal{J}^{bc} \\ \mathcal{J}^{cb} & \mathcal{J}^{cc} \end{bmatrix} \begin{bmatrix} \boldsymbol{q} \\ \boldsymbol{f} \end{bmatrix} = \begin{bmatrix} \boldsymbol{U} \\ \boldsymbol{U} \end{bmatrix}. \tag{20}$$

The drag force is then computed by

$$\boldsymbol{F} = \int \boldsymbol{q} dA + \sum_i^N \int \boldsymbol{f} ds_i. \tag{21}$$

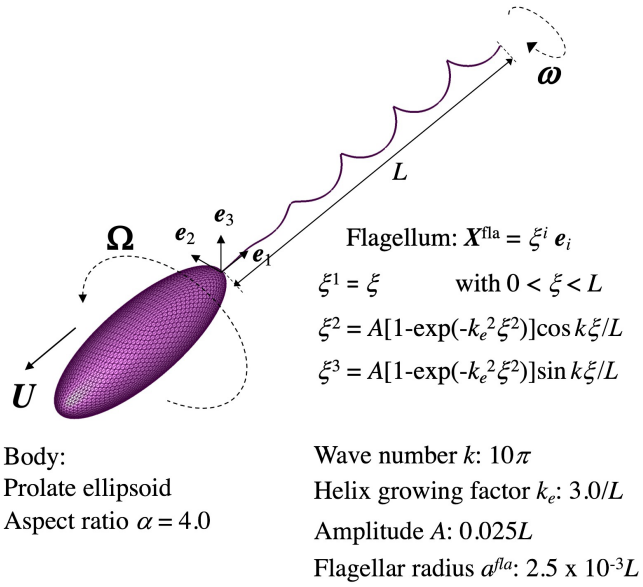

Fig.S 1. Bacterial model; geometrical data is obtained from Giacche et al. (4).

Bacteral model. We developed a bacterial model with the same manner as Giacche et al. (4). The bacterium body is expressed by a prolate spheroid with the aspect ratio $\alpha = a/b = 4$, where a and b are major and minor radii of the prolate body, respectively. The flagellum is assumed to be a cylindrical filament of cross-sectional radius a_f that executes helical waves. The flagellar waveform is prescribed, and the flagellum is assumed to rotate rigidly with constant angular velocity $\boldsymbol{\omega}$ relative to the cell body:

$$\begin{aligned} \boldsymbol{v}(\boldsymbol{x}) &= \boldsymbol{U} + \boldsymbol{\Omega} \wedge \hat{\boldsymbol{r}}(\boldsymbol{x}), && \boldsymbol{x} \in \text{cell body} \\ \boldsymbol{v}(\boldsymbol{x}) &= \boldsymbol{U} + (\boldsymbol{\Omega} - \boldsymbol{\omega}) \wedge \hat{\boldsymbol{r}}(\boldsymbol{x}), && \boldsymbol{x} \in \text{flagellum} \end{aligned} \quad [22]$$

where $\boldsymbol{U}$ is the translational velocity, and $\boldsymbol{\Omega}$ is the angular velocity. We seek unknowns $\boldsymbol{U}$ and $\boldsymbol{\Omega}$ under prescribed $\boldsymbol{\omega}$.

We define an orthonormal body frame $\boldsymbol{e}_i$ with its origin at the body-flagellum joint and the $\boldsymbol{e}_1$ axis coincides with the geometrical axis of the bacterium as depicted in Fig. S1. Then, flagellar shape $\boldsymbol{x}^{fla}(= \xi_i \boldsymbol{e}_i)$ is determined by

$$\boldsymbol{x}^{fla}(\xi) = \begin{pmatrix} \xi_1 = \xi, \\ \xi_2 = A[1 - \exp(-k_e^2 \xi^2)] \cos(k\xi/L), \\ \xi_3 = A[1 - \exp(-k_e^2 \xi^2)] \sin(k\xi/L), \end{pmatrix} \quad [23]$$

with $0 \leq \xi \leq L$. L is the length of the helix, $A = 0.025L$ is the amplitude, $k_e = 3.0/L$ is the helix growing factor, and $k = 10\pi$ is the wave number. The flagellar radius a_f is set as $a_f/L = 2.5 \times 10^{-3}$.

Sperm model. A sperm model was developed with the same methodology of Omori and Ishikawa (5). The geometry of human and bull sperm is likened to an asymmetric ellipsoid (cf. Fig. S2). To mimic the elliptical sperm head, the following mapping function is used:

$$X_1^{sp} = X_1,\ X_2^{sp} = \frac{aX_2}{a + b - X_1/\ell},\ X_3^{sp} = \frac{X_3}{c + X_1/\ell}, \quad [24]$$

where $\boldsymbol{X}^{sp}$ is the surface area of the sperm head, $\boldsymbol{X}$ is the material point of a sphere with radius ℓ, and a, b, and c are non-dimensional shape parameters. The parameters are set as, $\ell/L = 4.17 \times 10^{-2}$, $a = 3.0$, $b = 2.0$, and $c = 4.0$, to ensure that the morphology is similar to that of human sperm cells.

The flagella beat for a human and bull sperm show a left-handed helicoid. To express the time-dependent flagellum, the following formula can be used

$$\begin{aligned} \xi_2 &= A\cos(k\xi/L - 2\pi t/T), \\ \xi_3 &= -\alpha A \sin(k\xi/L - 2\pi t/T), \end{aligned} \quad [25]$$

where L is the flagellum length, T is the period, k is wave number, A is the amplitude parameter, and $\alpha = 0.2$ is helix parameter. The wave number and amplitude parameter are set as $k/\pi = 2.0$, and $A = 0.1087\xi_1$. To coincide with a human sperm flagellum, the flagellar radius $a_f/L = 2.35 \times 10^{-3}$ is used. Prescribed velocity of the flagellum is given by $\boldsymbol{v}^{fla} = \partial\xi_2/\partial t\ \boldsymbol{e}_2 + \partial\xi_3/\partial t\ \boldsymbol{e}_3$, and is substituted to Eq.[17]. We then solve the system with respect unknowns $\boldsymbol{U}$, $\boldsymbol{\Omega}$, $\boldsymbol{q}$ and $\boldsymbol{f}$.

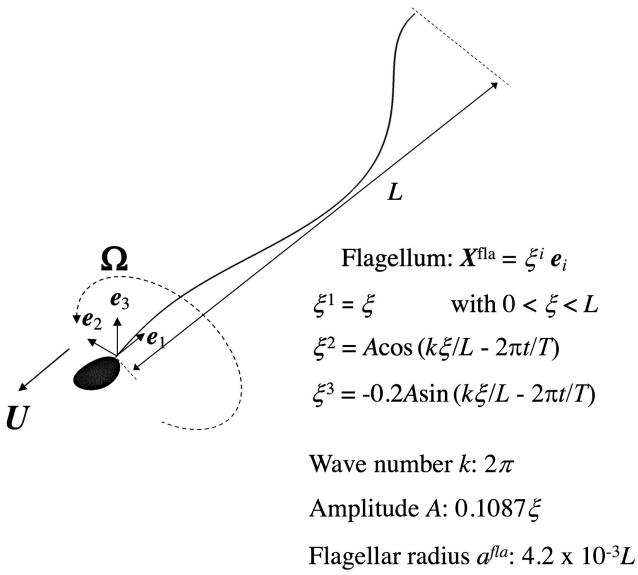

Fig.S 2. Sperm model; geometrical data is obtained from Omori and Ishikawa (5).

Supplemental data

Flow field around a spherical ciliate with in-phase beating. Flow filed around a spherical ciliate, $a/L = 10$, and $N = 636$ is shown in Fig. S3(a), where a is the radius, L is the cilium length, and N is the number of cilia. The swimming velocity U and mechanical power P with $N = 162$, 636, and 2520 are also shown in the Figures S3(b) and (c), respectively.

Flow field around an ellipsoidal ciliate. Flow filed around a prolate ciliate with the aspect ratio $\alpha(= a/b) = 2$ is shown in Figs. S4, S5, and S6, where a is the major axis, and b is the minor axis of the ellipsoid. The body shape is controlled to hold the volume constant regardless of the aspect ratio. Results of three types of metachronal wave are shown in the Figures; antiplectic is shown in Fig. S4, symplectic is S5, and in-phase beating is shown in Fig. S6. The swimming velocity U and mechanical power P with $N = 162$, 636, and 2520 are also shown in the Figures.

Swimming velocity as a function of number of cilia. Time-averaged swimming velocity with various body size and aspect ratio is shown in Fig. S7. In all cases, the swimming speed U can be scaled as $U \propto N$.

Mechanical power as a function of number of cilia. Time-averaged power with various body size and aspect ratio is shown in Fig. S8. In all cases, the mechanical P can be scaled as $P \propto N$.

Swimming efficiency as a function of number of cilia. Swimming efficiency with various body size, number of cilia, and metachronal waves are shown in Fig. S9.

Effects of ciliary placement. We compared two different distribution of cilia; (a) homogeneous distribution, and (b) arranged in the spherical coordinate, as shown Fig. S10. In the spherical coordinate, we define the number of cilia both in the longitude and latitude directions,N_θ, and N_ϕ, and the result is shown in Fig. S11. The radius a is set as $a/L = 5$, and we set symplectic mode. We see that the efficiency can be changed by the ciliary distribution even when the number of cilia is constant. The maximum efficiency is given by $N = 216$ ($N_\theta = 12$ and $N_\phi = 18$), and cilia are distributed almost homogeneous. In this case, the optimal interval among surface cilia can be $\Delta r^{opt}/L = 1.2$, which corresponds to the result of homogeneously distributed cilia (cf. Fig.4c in the main text). We then investigated the effect of body size and optimal number of cilia (cf. Fig. S12). We confirmed the maximum efficiency is given when cilia are distributed homogeneously, and the resultant maximum efficiency is similar to that of homogeneously distributed cilia. In Fig. S12(b), we can see the optimal number of cilia is proportional to $(a/L)^2$ both in the spherical coordinate and homogeneous cases. From these results, we conclude the optimal efficiency is given when cilia are distributed homogeneously.

1. Ito H, Omori T, Ishikawa T (2019) Swimming mediated by ciliary beating: Comparison with a squirmer model. *J. Fluid Mech.* 874:774–796.
2. Tornberg AK, Shelly MJ (2004) Simulating the dynamics and interactions of flexible fibers in stokes flows. *J. Comput. Phys.* 196:8–40.
3. Fulford GR, Blake JR (1986) Muco-ciliary transport in the lung. *J. Theor. Biol.* 121:381–402.
4. Giacche D, Ishikawa T, Yamaguchi T (2010) Hydrodynamic entrapment of bacteria swimming near a solid surface. *Phys. Rev. E* 82:056309.
5. Omori T, Ishikawa T (2016) Upward swimming of a sperm cell in shear flow. *Phys. Rev. E* 93:032402.

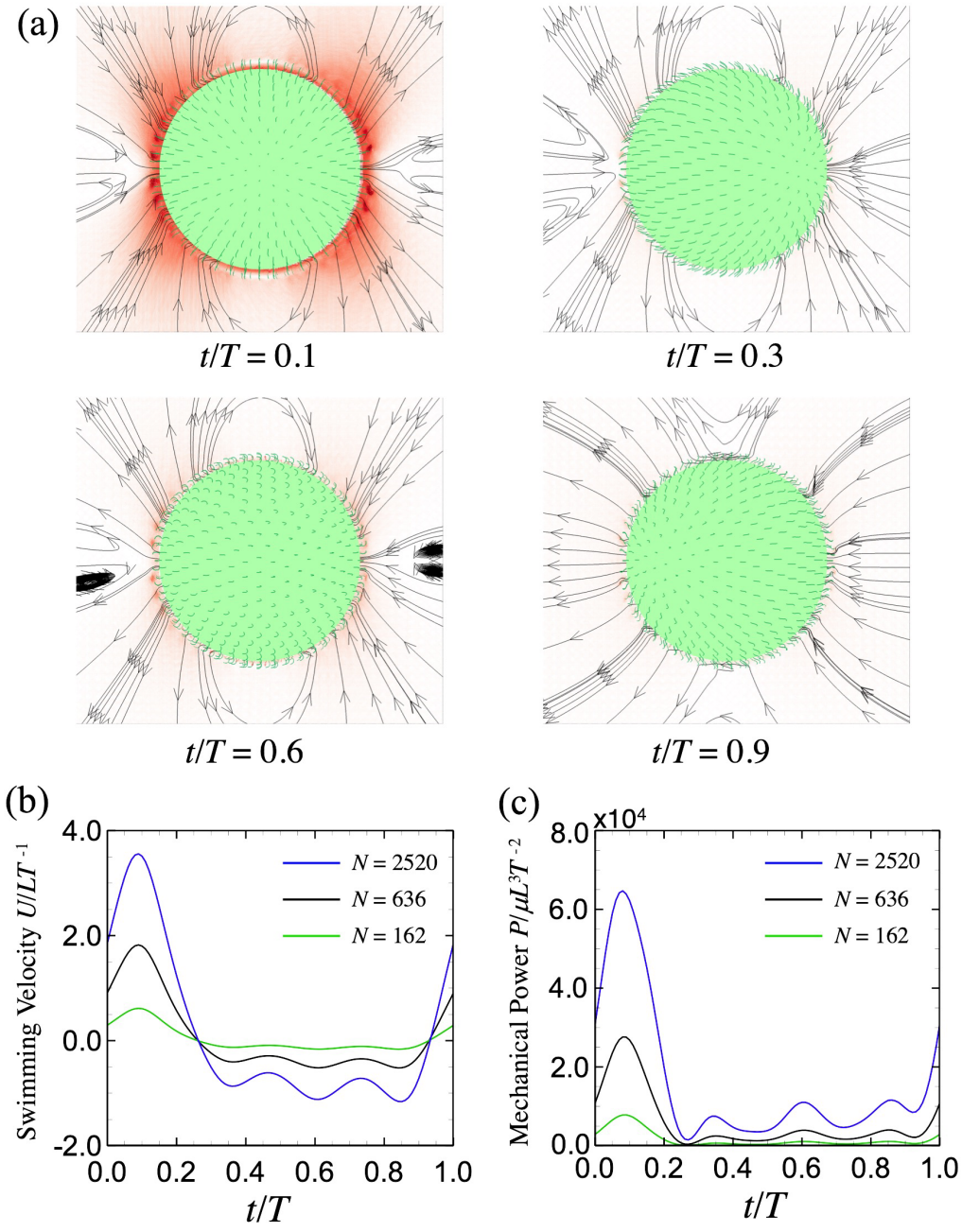

Fig.S 3. Ciliate with in-phase beating. (a) Flow field around the ciliate, Red indicates flow magnitude (b) Time change of swimming velocity and (c) power generated by the ciliate. μ is the viscosity, T is the period, L is the length of cilium, and N is the number of cilia.

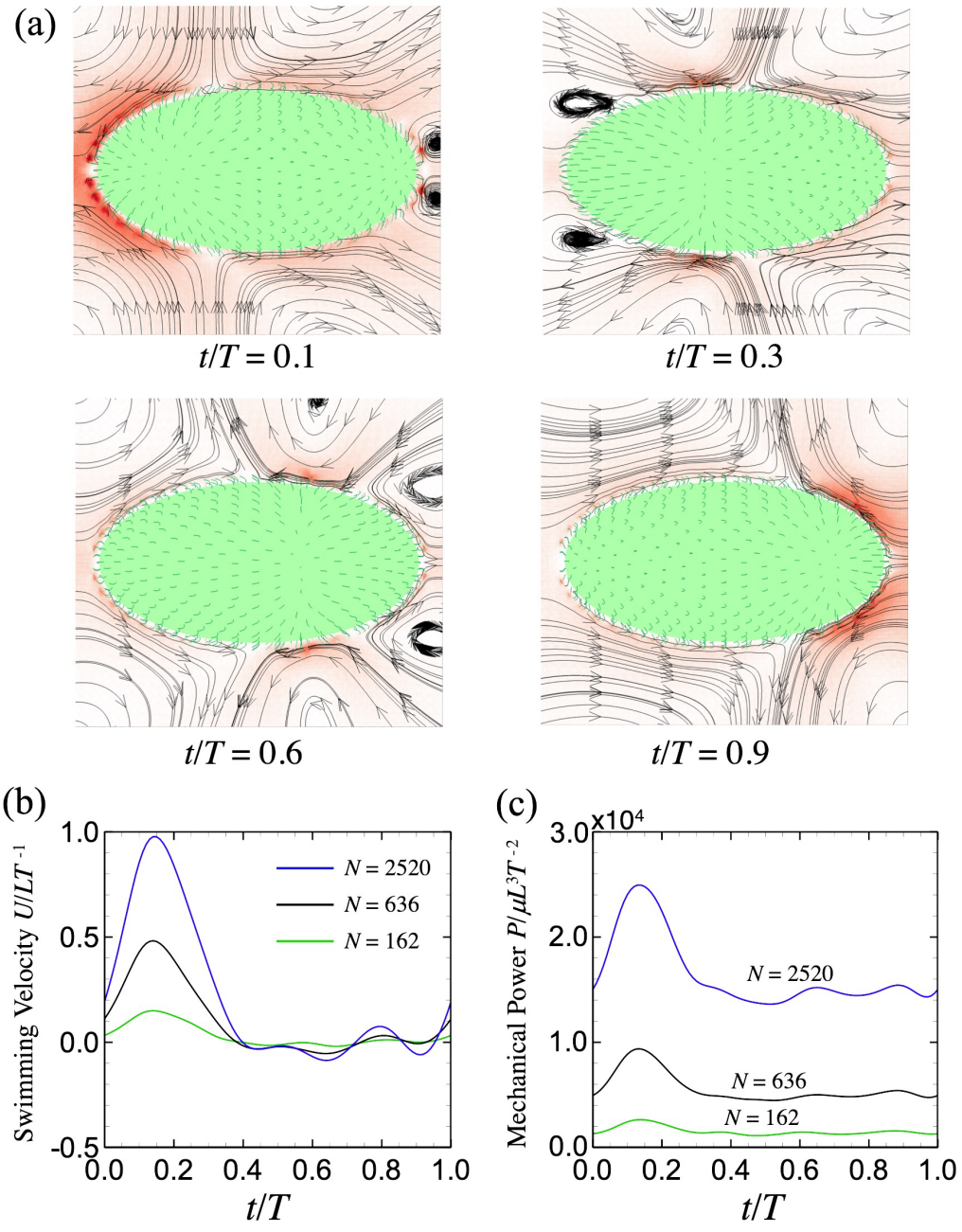

Fig.S 4. Prolate ciliate with antiplectic beating. The aspect ratio α = 2.0. (a) Flow field around the ciliate, Red indicates flow magnitude (b) Time change of swimming velocity and (c) power generated by the ciliate.

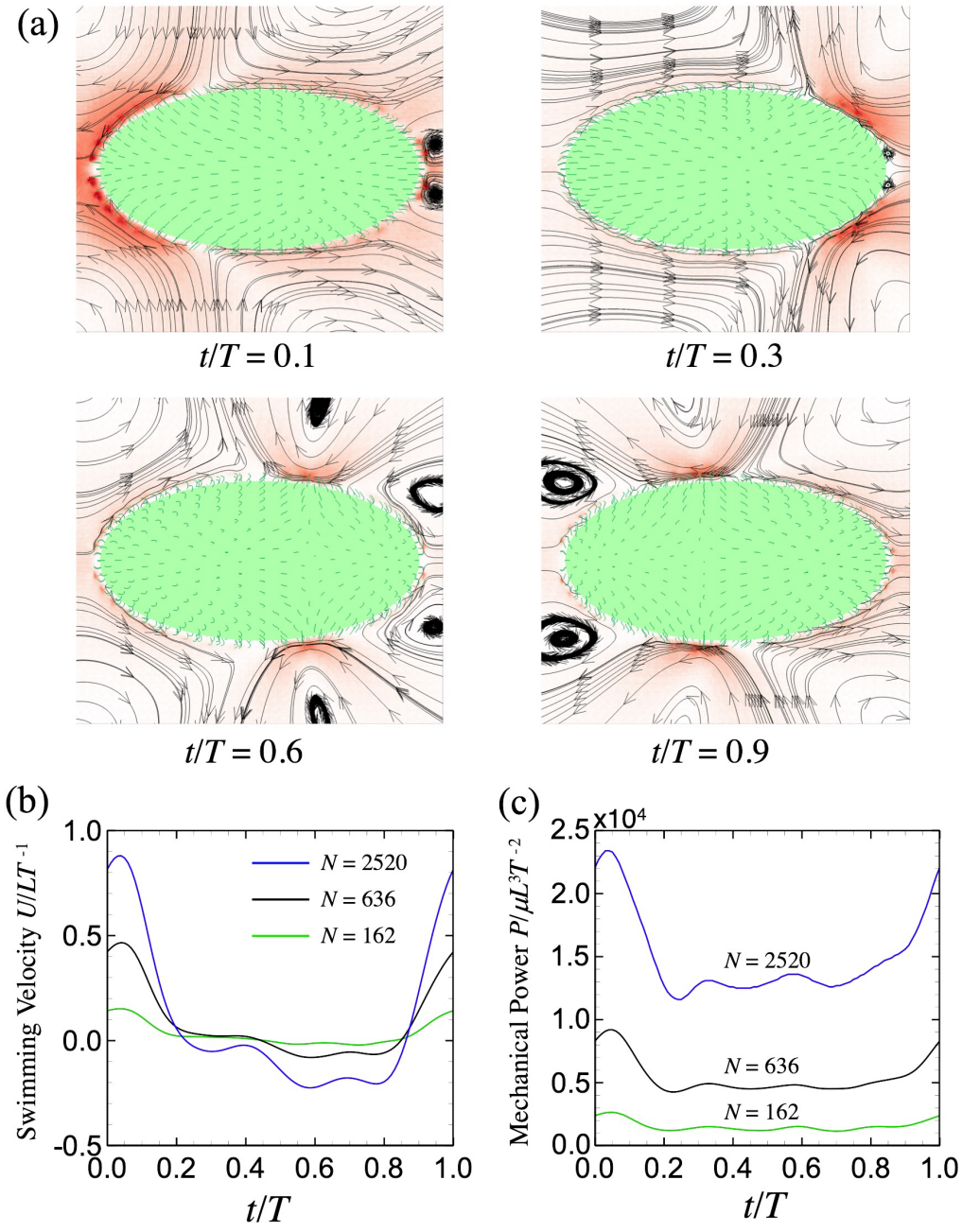

Fig.S 5. Prolate ciliate with symplectic beating. The aspect ratio α = 2.0. (a) Flow field around the ciliate, Red indicates flow magnitude (b) Time change of swimming velocity and (c) power generated by the ciliate.

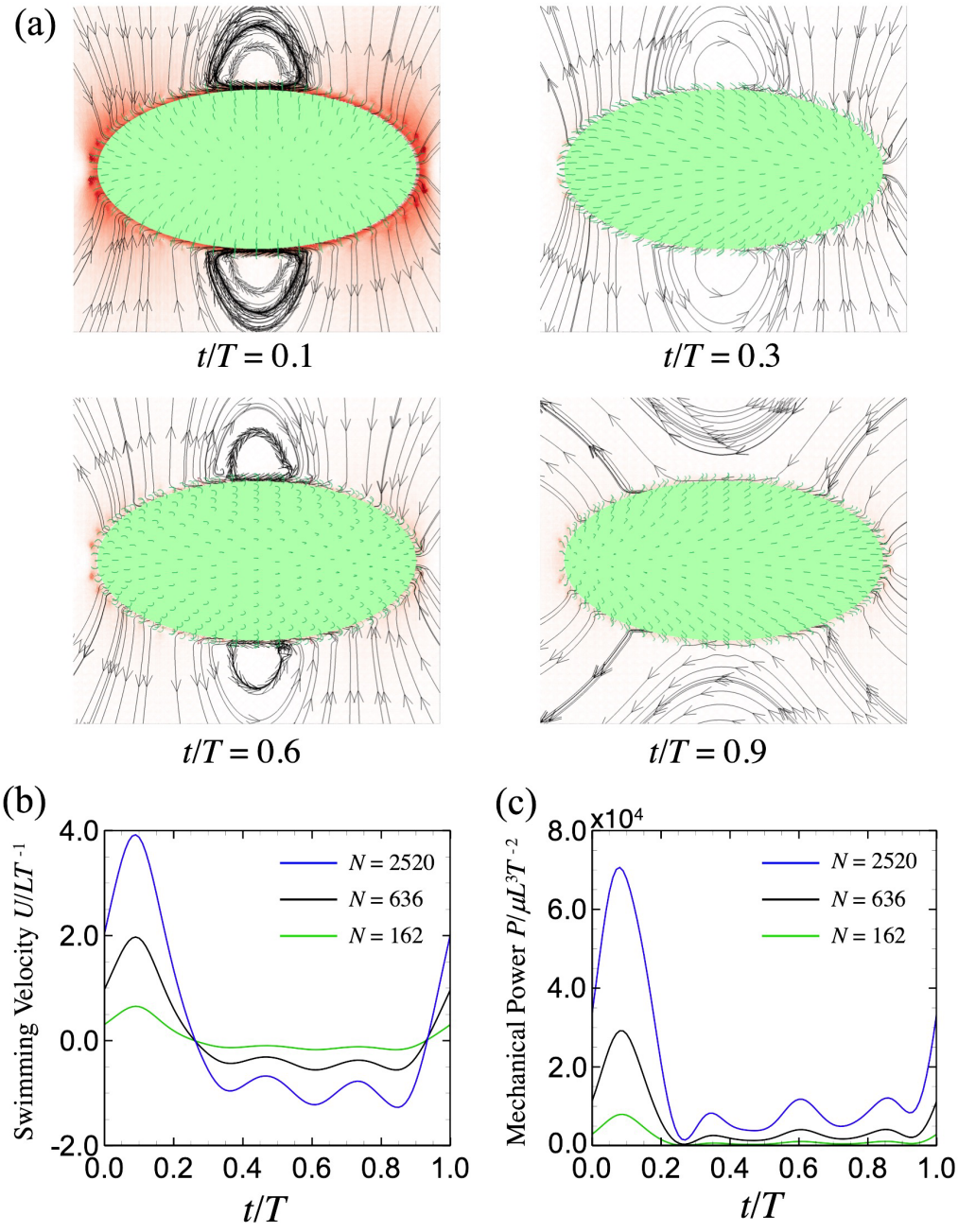

Fig.S 6. Prolate ciliate with in-phase beating. The aspect ratio α = 2.0. (a) Flow field around the ciliate, Red indicates flow magnitude (b) Time change of swimming velocity and (c) power generated by the ciliate.

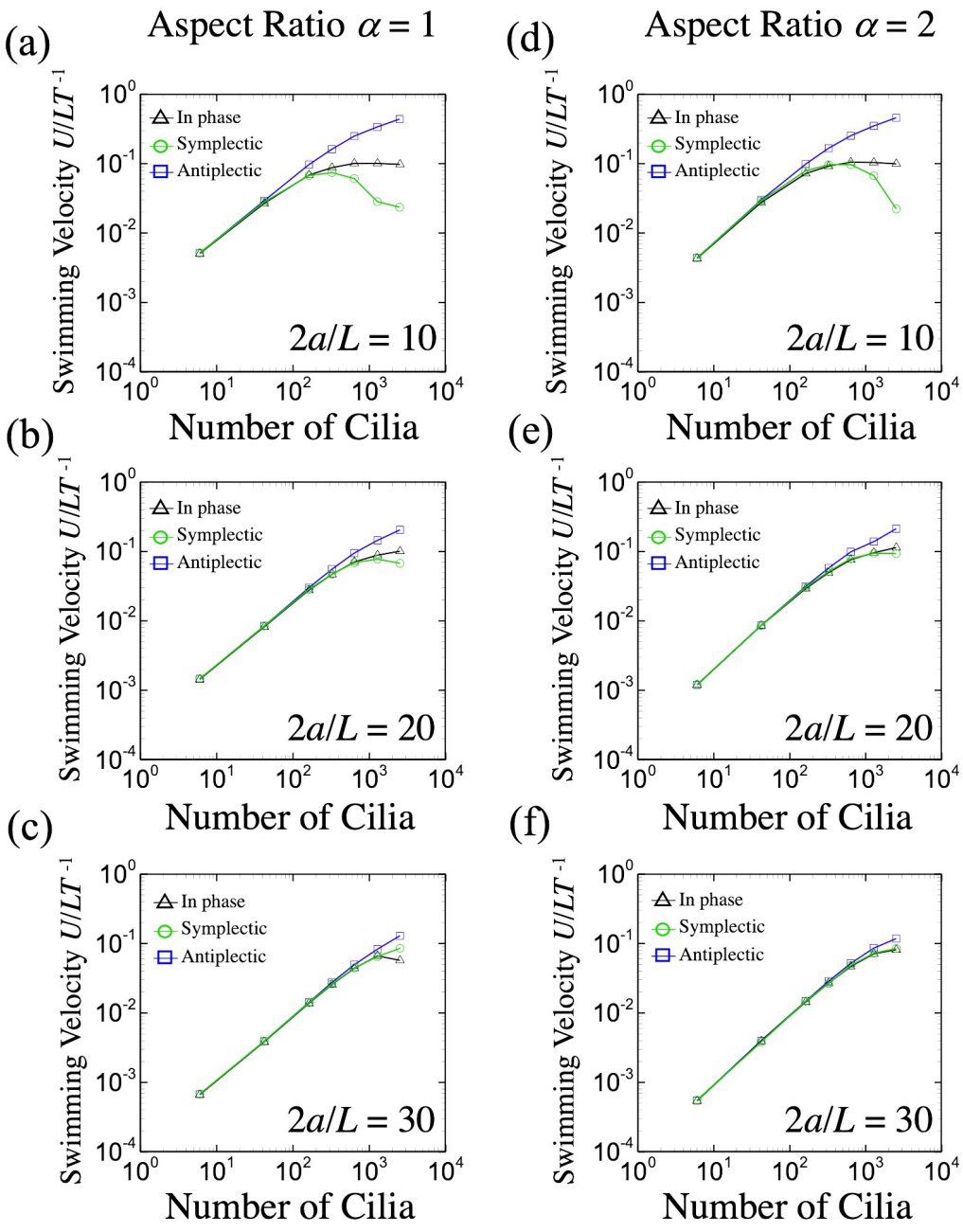

Fig.S 7. Time averaged swimming velocity as a function of number of cilia with three types of metachronal waves (in-phase; triangle, symplectic; circle; and antiplectic; square); (a-c) the results of α = 1.0 and (d-f) α = 2.0.

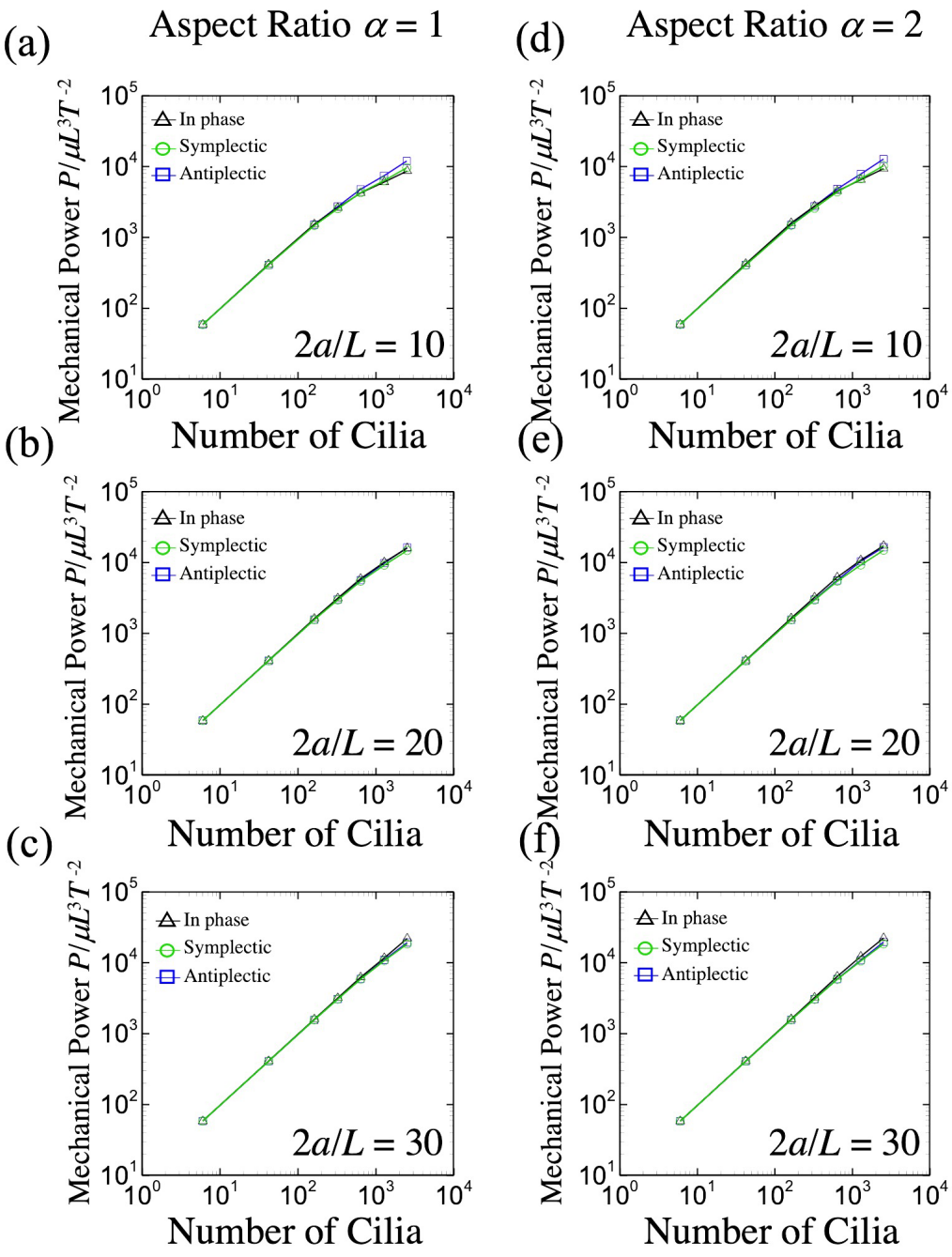

Fig.S 8. Time averaged mechanical power as a function of number of cilia with three types of metachronal waves (in-phase; triangle, symplectic; circle; and antiplectic; square); (a-c) the results of α = 1.0 and (d-f) α = 2.0.

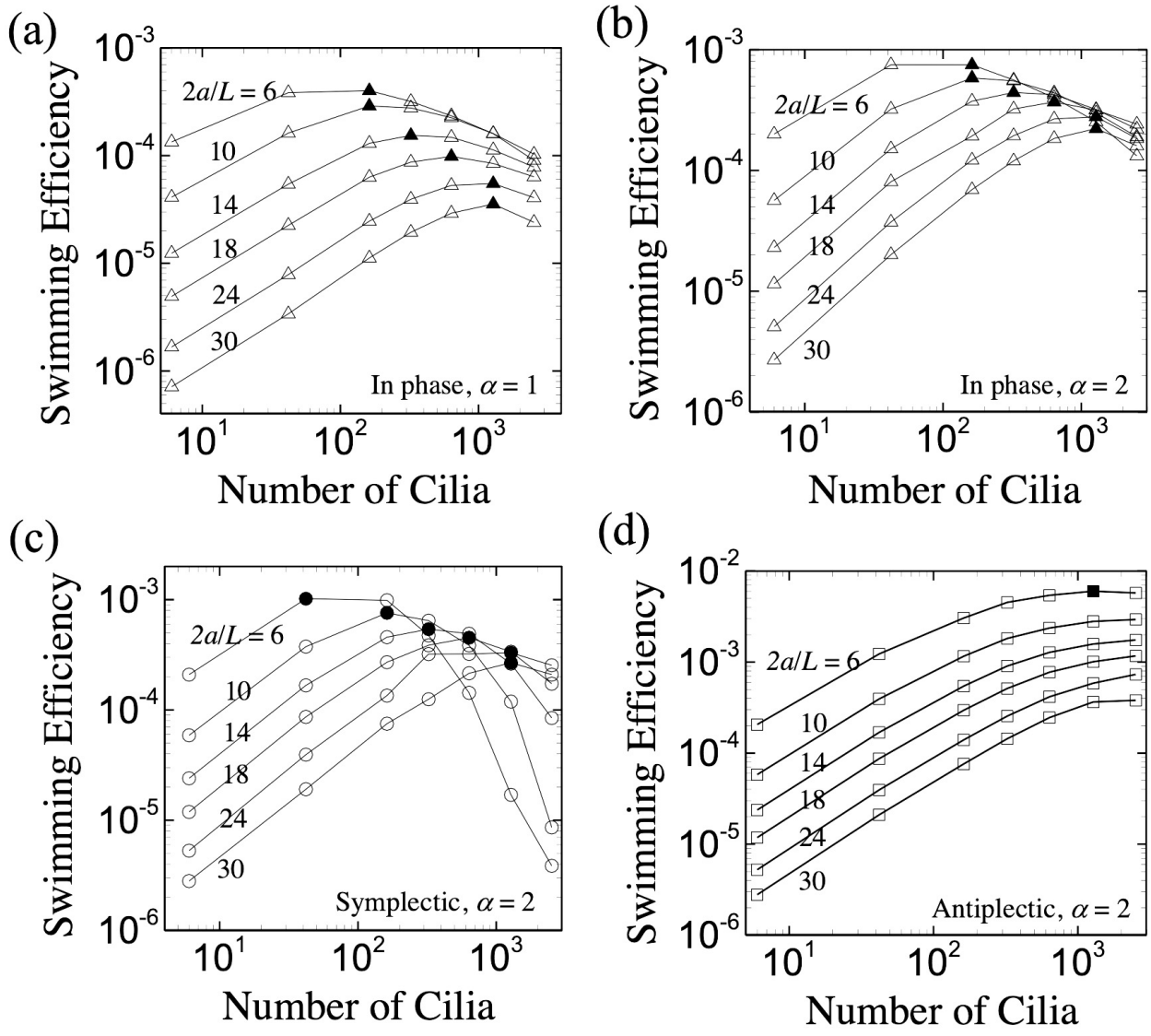

Fig.S 9. Swimming efficiency with various body radius a, aspect ratio α, and metachronal waves; (a) in-phase and spherical ciliate, (b) in-phase, prolate ciliate, (d) symplectic, prolate ciliate, and (e) antiplectic, prolate. Filled symbols indicate the maximum efficiency in each case.

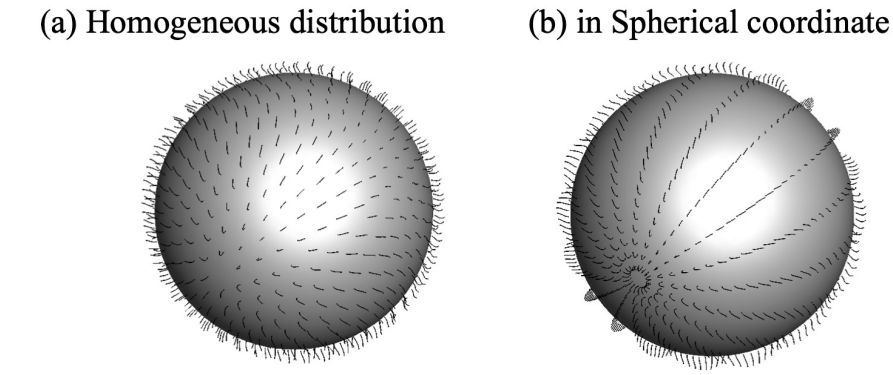

Fig.S 10. Placement of cilia (a) homogeneous distribution and (b) arranged in the spherical coordinate.

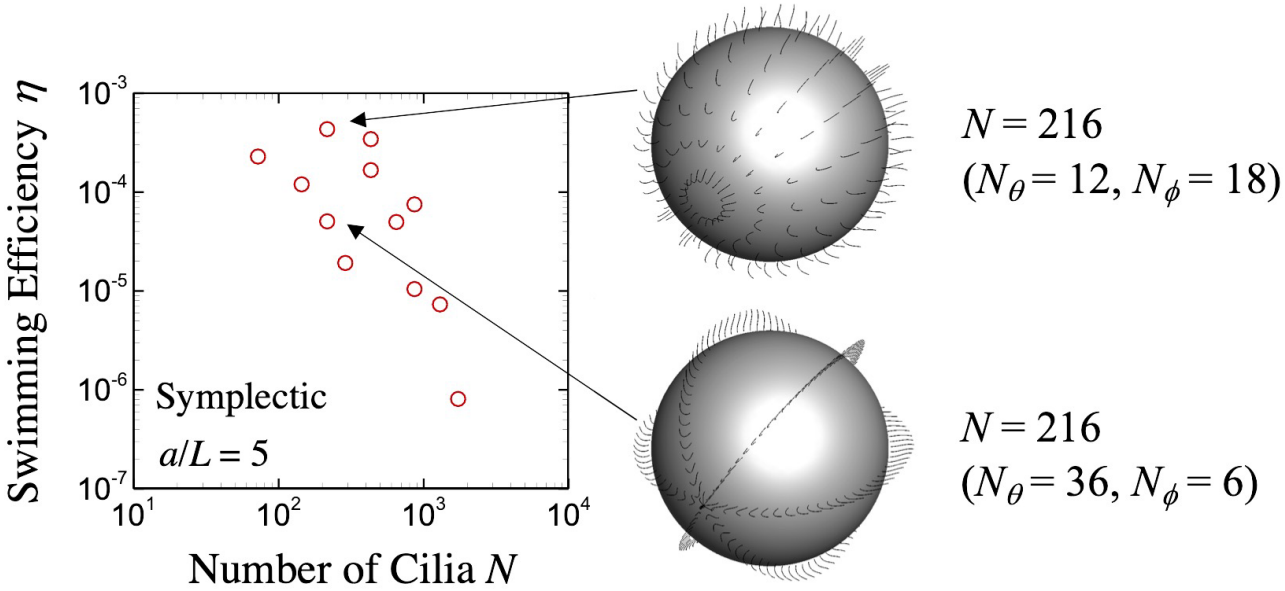

Fig.S 11. Swimming efficiency with various ciliary distributions (the body radius $a/L = 5$ and symplectic mode). L is the cilium length, θ and ϕ indicate the longitude and latitude directions, respectively.

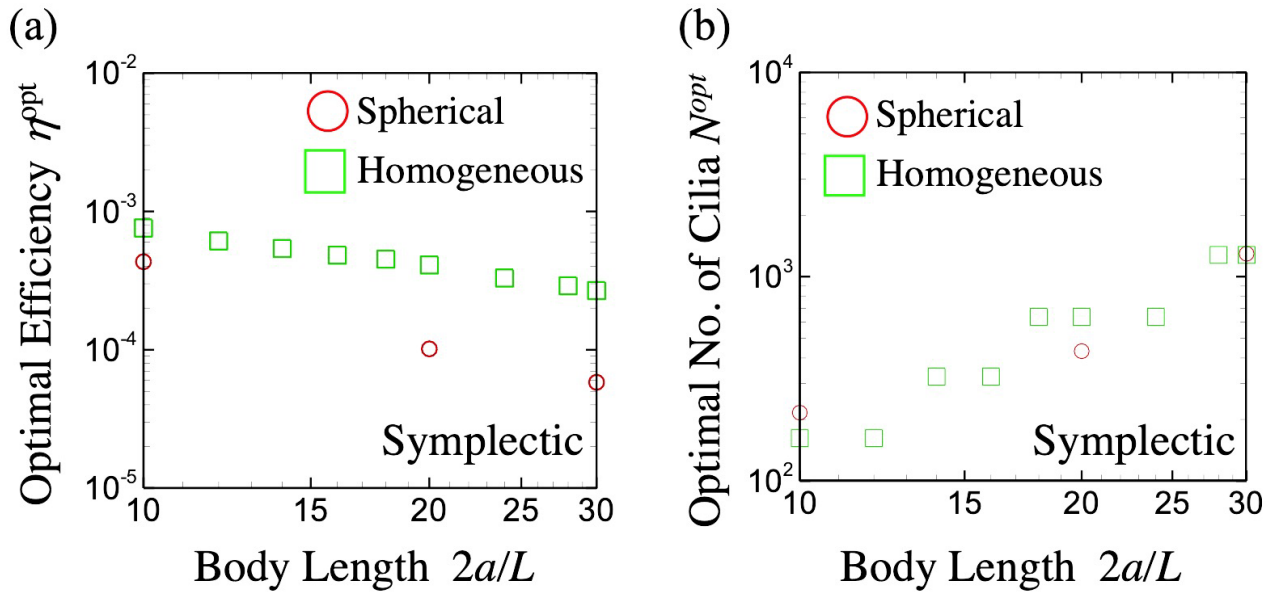

Fig.S 12. Optimal efficiency and number of cilia with different ciliary distribution